RESEARCH

Single-cell transcriptomics of hepatic stellate cells uncover crucial pathways and key regulators involved in non-alcoholic steatohepatitis

Weiwei He[1,2,3,*], **Caoxin Huang**[2,3,*], **Xiulin Shi**[2,3,4], **Menghua Wu**[1,2,3], **Han Li**[1,2,3], **Qiuhong Liu**[1,2,3], **Xiaofang Zhang**[2,3], **Yan Zhao**[2,3] and **Xuejun Li**[2,3,4,5]

[1]School of Medicine, Xiamen University, Xiamen, China
[2]Xiamen Diabetes Institute, The First Affiliated Hospital of Xiamen University, Xiamen, China
[3]Fujian Provincial Key Laboratory of Translational Medicine for Diabetes, Xiamen, China
[4]Department of Endocrinology and Diabetes, The First Affiliated Hospital of Xiamen University, Xiamen, China
[5]Xiamen Clinical Medical Center for Endocrine and Metabolic Diseases, Xiamen Diabetes Prevention and Treatment Center, Xiamen, China

Correspondence should be addressed to X Li or Y Zhao: lixuejun@xmu.edu.cn or zhaoyan1976@126.com

*(W He and C Huang contributed equally to this work)

Abstract

Background: Fibrosis is an important pathological process in the development of non-alcoholic steatohepatitis (NASH), and the activation of hepatic stellate cell (HSC) is a central event in liver fibrosis. However, the transcriptomic change of activated HSCs (aHSCs) and resting HSCs (rHSCs) in NASH patients has not been assessed. This study aimed to identify transcriptomic signature of HSCs during the development of NASH and the underlying key functional pathways.

Methods: NASH-associated transcriptomic change of HSCs was defined by single-cell RNA-sequencing (scRNA-seq) analysis, and those top upregulated genes were identified as NASH-associated transcriptomic signatures. Those functional pathways involved in the NASH-associated transcriptomic change of aHSCs were explored by weighted gene co-expression network analysis (WGCNA) and functional enrichment analyses. Key regulators were explored by upstream regulator analysis and transcription factor enrichment analysis.

Results: scRNA-seq analysis identified numerous differentially expressed genes in both rHSCs and aHSCs between NASH patients and healthy controls. Both scRNA-seq analysis and *in-vivo* experiments showed the existence of rHSCs (mainly expressing a-SMA) in the normal liver and the increased aHSCs (mainly expressing collagen 1) in the fibrosis liver tissues. NASH-associated transcriptomic signature of rHSC (NASHrHSCsignature) and NASH-associated transcriptomic signature of aHSC (NASHaHSCsignature) were identified. WGCNA revealed the main pathways correlated with the transcriptomic change of aHSCs. Several key upstream regulators and transcription factors for determining the functional change of aHSCs in NASH were identified.

Conclusion: This study developed a useful transcriptomic signature with the potential in assessing fibrosis severity in the development of NASH. This study also identified the main pathways in the activation of HSCs during the development of NASH.

Keywords

- non-alcoholic steatohepatitis
- hepatic stellate cell
- fibrosis

Endocrine Connections (2023) **12**, **e220502**

https://ec.bioscientifica.com
https://doi.org/10.1530/EC-22-0502

Introduction

Non-alcoholic fatty liver disease (NAFLD), as the main liver disease manifestation of metabolic diseases, is closely related to obesity, insulin resistance, type 2 diabetes, and dyslipidemia (1, 2). With the improvement of living standards and changes in lifestyles, the incidence of NAFLD has been increasing worldwide, and it has become one of the most important causes of chronic liver dysfunction (2, 3). NAFLD ranges from simple steatosis to nonalcoholic steatohepatitis (NASH), which is characterized by the ballooning of hepatocytes and inflammation (4, 5, 6). NAFLD is now the most common chronic liver disease with a global prevalence of nearly 25%, while the global prevalence of NASH is estimated at 3% to 5% and NASH is the second leading cause of liver transplantation and poses a heavy financial burden (7, 8, 9).

Fibrosis is a major determinant of clinical outcome in patients with NASH and is associated with an increased risk of cirrhosis and liver cancer (10, 11, 12). In addition, the occurrence of liver fibrosis is a significant predictor of all-cause and liver-related disease mortality in NAFLD, and the risk of liver-related mortality increases exponentially with higher fibrosis stages (13, 14). However, there is lack of effective treatments for fibrosis in NASH (15). Therefore, it is important to explore the mechanisms of liver fibrosis of NASH and uncover the key treatment targets. Liver fibrosis is mainly characterized by the overproduction and deposition of extracellular matrix (ECM) (16). Under normal condition, ECM produced by hepatic stellate cells (HSCs) during liver injury and tissue repair can be hydrolyzed by matrix metalloproteinases (MMPs). However, an imbalance between ECM synthesis and degradation can lead to the development of liver fibrosis (16, 17, 18). Activation of the HSCs is currently regarded as a central event in liver fibrosis (19, 20). Studies over the last two decades have shown that myofibroblasts (MFBs) are the main cells producing ECM during various chronic liver injuries, while HSCs remain the main source of MFBs in various clinical and experimental liver fibrosis models (21, 22, 23). HSCs can transform into MFBs and express α-SMA in large quantities, and this transformation is a key event in the progression of liver fibrosis (24).

NASH-related fibrosis is an important pathological process in the progression of NAFLD, but the risk of developing fibrosis cannot be predicted by liver tissue biopsy. Fibrosis is an important pathological process in the development of NASH, and the activation of HSC is a central event in liver fibrosis. However, the transcriptomic change of activated HSCs (aHSCs) and resting HSCs (rHSCs) in NASH patients has not been assessed. In this study, we analyzed the single-cell RNA-sequencing (scRNA-seq) data of liver tissues from NASH patients and healthy controls. This study aimed to identify the transcriptomic signature of HSCs during the development of NASH and the underlying key functional pathways.

Materials and methods

scRNA-seq data of NASH and healthy control liver tissues

scRNA-seq data of NASH and healthy control liver tissues from Gene Expression Omnibus (GEO) were analyzed in our study. The data were from GSE136103 (Supplementary Table 1, see section on supplementary materials given at the end of this article). The Seurat package was used in the scRNA-seq analyses, and SCTtransform approach was used in integrating data from multiple samples (25). Cells were clustered with both uniform manifold approximation and projection (UMAP) and t-distributed stochastic neighbor embedding (t-SNE) methods, and the types of cell clusters were defined with previously defined makers of distinct cells. The signature genes highly expressed in each cluster but not in the other clusters were identified with Seurat package, and the differentially expressed genes (DEGs) of HSCs between NASH patients and controls were further calculated.

Transcriptomic profile datasets

We searched the transcriptomic profile datasets of liver tissues from NAFLD patients in GEO. Ultimately, GSE49541, GSE126848, and GSE130970 were included as validation datasets of our study, and all those three datasets were transcriptomic profile datasets of liver tissues from NAFLD patients. In addition, we used GSE148849, a transcriptomic dataset of HSC stimulated by TGF-β *in vitro*, to assess the changes of NASH-related signature gene sets during HSCs activation. DESeq2 of R package was used to determine DEGs for RNA-sequencing (RNA-seq) datasets, and limma package was used to determine DEGs for microarray datasets. We further validated the major findings from scRNA-seq analyses by bulk RNA-seq data containing 206 patients with NAFLD and further evaluated the clinical significance of key transcriptomic signatures (GSE135251). The characteristics of those publicly available transcriptomic datasets used in the analysis are shown Supplementary Table 2.

https://ec.bioscientifica.com
https://doi.org/10.1530/EC-22-0502

Gene set variation analysis

Gene set variation analysis (GSVA) is a non-parametric unsupervised analysis method mainly used to evaluate the results of gene set enrichment in transcriptomes (26). To verify the enrichment of the HSC-related signature gene sets in scRNA-seq data, we used GSM4041162 for GSVA. In addition, to verify the enrichment of the signature gene set for TGF-β stimulated HSC activation, we used GSE148849 for GSVA.

Gene set enrichment analysis

Gene set enrichment analysis (GSEA) is a computational method that determines whether an *a priori*-defined set of genes shows statistically significant and consistent differences between two biological states (27). To determine the enrichment of the signature gene set for TGF-β-stimulated HSC activation, we used GSE148849 for GSEA. In addition, to explore the enrichment of the signature gene sets developed above in the differentially expressed genes (DEGs) list for the progression from NAFL to NASH or fibrosis progression, we also performed GSEA using data from our previous study (28).

Weighted gene co-expression network analysis

To further clarify the possible functional pathways related to the enrichment of signature gene sets, weighted gene co-expression network analysis (WGCNA) was further performed using the R package 'WGCNA'. WGCNA is a systematic method used to describe the gene co-expression patterns between different samples that can be used to identify highly synergistic co-expression modules (29). GSE49541 was used in this study including 72 patients with NAFLD.

Upstream regulator and transcription factor analyses

In this study, we further explored those key regulators or transcription factor analyses for determining the functional change of aHSCs in NASH. To infer the upstream regulators from the DEGs in aHSCs between NASH and controls, quaternary test statistical analyses were performed with the R package of QuaternaryProd (30). To identify those transcription factors for determining the functional change of aHSCs in NASH, transcriptional regulatory networks of those DEGs in aHSCs between NASH and controls were explored with the Cytoscape plugin of iRegulon, which could detect enriched transcription factor motifs and their direct targets (31).

Experimental animals

C57L/J male mice were obtained from Xiamen University Experimental Animal Center. Mice were fed standard rodent chow *ad libitum* and housed on woodchip beds. Mice were randomly divided into NASH group and control group at 12 weeks of age. The NASH mice model group was fed a high-fat and choline methionine-deficient diet (HFMCD) (A06071301B16; Research Diets, New Brunswick NJ) for 10 weeks. The control mice were fed standard rodent chow *ad libitum*.

DBA/2J mice were purchased from Beijing Vital River Laboratory Animal Technology Co., Ltd. and were placed in the Xiamen University Experimental Animal Center. Mice were administered intraperitoneally at a dose of 5 μL of 10% CCl4 olive oil solution per gram of body weight. CCl4 injections were started at 12 weeks of age, twice a week for 6 weeks. Olive oil was used in control mice.

Histological examination

The liver specimens of each group were fixed in 10% buffered neutral formalin for 24 h. The fixed specimens were routinely processed to obtain 4–5 μm thick paraffin sections for histological and immunohistochemical evaluation. Sections of each group were stained with Masson trichrome and hematoxylin and eosin (H&E) stain. Collagen 1 (1:200, ab5694, Abcam) and anti-a-SMA (1:200, 72026T, CST) were used for immunohistochemical staining. The samples were then observed and photographed under a microscope. For immunofluorescence staining, liver sections were stained with FITC fluorescent anti-a-SMA antibody (72026T, CST) and cy3 fluorescent anti-collagen 1 antibody (ab5694, Abcam). Nuclei were then stained with DAPI, and the liver sections were then observed and photographed using a fluorescence microscope.

Statistical analysis

Expressions of key genes in liver tissues were presented with median and interquartile range, and difference between advanced fibrosis liver tissues and mild fibrosis liver tissues was determined with Mann-Whitney *U* test. Difference in the enrichment scores from GSVA between groups was determined with unpaired *t*-test. The performance of enrichment scores from GSVA in diagnosing fibrosis or NASH among NAFLD patients

https://ec.bioscientifica.com
https://doi.org/10.1530/EC-22-0502

was explored by receiver operating characteristic (ROC) analysis and area under the curve (AUC) was calculated. R software (version 3.6.1) was used in statistical analyses. $P < 0.05$ was considered to be significant.

Results

Single-cell transcriptomics in liver identified HSCs subset-specific transcriptomic signatures

A total of six liver samples of single-cell transcriptomics were included in our study, and they were GSM4041151, GSM4041156, GSM4041157, GSM4041159, GSM4041162, and GSM4041163. The main characteristics of these samples are shown in Supplementary Table 1. These six samples contained four healthy controls and two NAFLD samples with fibrosis. After integration by SCTtransform approach, scRNA-seq analyses were subsequently performed. Those cells were classified into 19 clusters by the tSNE or UMAP algorithm (Fig. 1A and B). Two main HSCs subsets including aHSC and rHSC were identified, and they were both identified in the liver tissues of NASH patients and healthy controls (Fig. 1C).

Through scRNA-seq analyses, we further identified the signature genes expressed by each cell cluster. The signature genes of aHSC and rHSC are shown in Table 1. For instance, rHSCs highly expressed RGS5, NDUFA4L2, MYH11, RERGL, etc., and aHSC highly expressed LUM, COL3A1, DPT, PCOLCE, etc. To facilitate the analysis of HSCs alterations using bulk transcriptomic data, we constructed the transcriptomic signature of activated HSC (aHSCsignature) and transcriptomic signature of resting HSC (rHSCsignature) based on the above results. The aHSCsignature consisted of top 54 genes that were highly expressed in aHSCs. rHSCsignature consisted of top 79 genes that were highly expressed in rHSCs (Table 1).

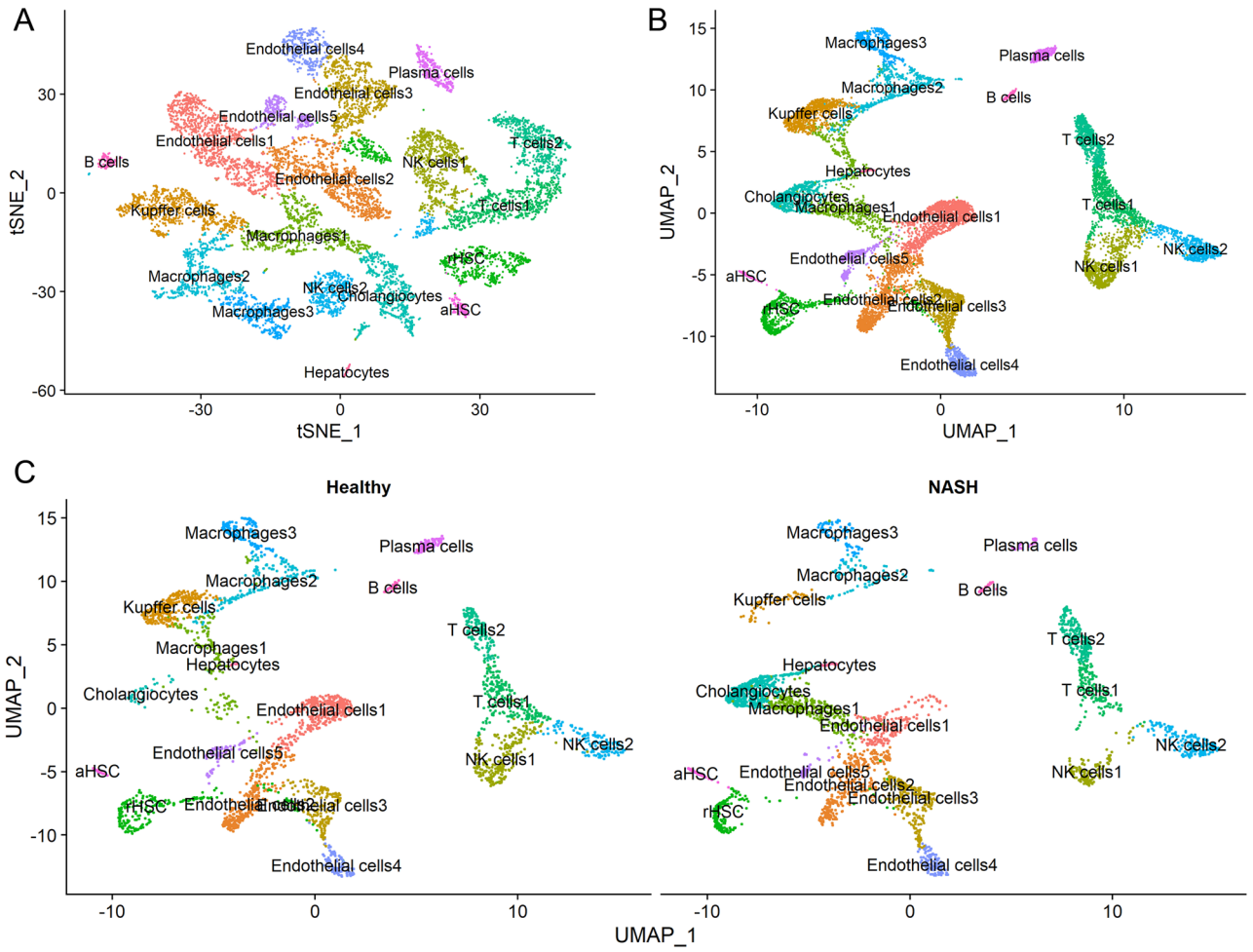

Figure 1

Single-cell transcriptomics of liver tissues identified HSCs subsets and the transcriptomic signatures (A, t-SNE plot of cell clusters in liver tissues; B, UMAP plot of cell clusters in liver tissues; C, Comparative analysis cell clusters in liver tissues between NASH and healthy controls).

https://ec.bioscientifica.com
https://doi.org/10.1530/EC-22-0502

Table 1 Gene lists of the signature gene sets developed in this study

Gene signatures	Gene list
rHSCsignature	RGS5, NDUFA4L2, MYH11, RERGL, COX4I2, MAP3K7CL, RCAN2, NET1, PLN, NOTCH3, LMOD1, SERPINI1, PGF, C2orf40, RASD1, NTRK2, CNN1, KLHL23, TBX2, FOXS1, KCNK17, PPP1R12B, HIGD1B, EFHD1, RERG, NRGN, GPR20, GUCY1B3, RRAD, RBPMS2, LGI4, MRGPRF, MRVI1, HRC, CAP2, GRIP2, ACTG2, HEY2, FAM162B, MYOZ1, DMPK, EDNRA, ENPEP, VASN, ITGA7, NT5DC2, CDH6, PRKG1, ARHGEF25, SYNM, RASL12, NTRK3, PDGFA, FAM129A, CLMN, ARPC1A, SMIM10, PCSK7, AOC3, PTK2, MTHFD2, TTLL7, UBA2, GPRC5C, PPP1R12A, TMEM51, PHLDA2, HACD1, KCNMB1, SPECC1, HOXB2, GRK5, OAT, TLE1, ILK, PACSIN2, CCNI, PPP1R15A, ROCK1
aHSCsignature	LUM, COL3A1, DPT, PCOLCE, GGT5, ASPN, FBLN1, OLFML3, COL14A1, ITGBL1, COLEC10, ISLR, ADAMTSL2, PDGFRA, COL5A1, SFRP4, OGN, PODN, THBS2, GPC3, LOXL1, STMN2, LAMA2, ABCA8, COL5A2, CH25H, SAMD11, LAMC3, THY1, ADAMTS13, CXCL14, CYGB, ANGPTL6, CTSK, ADAMTS2, CLEC11A, GPC6, AGTR1, RCN3, COL6A3, CCBE1, CTHRC1, CRABP2, CCL19, PDLIM4, LAMB1, FGF7, FSTL3, FKBP10, CERCAM, QSOX1, CCDC146, CYBRD1, CTSF
NASHrHSCsignature	ID3, MALAT1, CRIP1, IGFBP7, MTRNR2L12, NDUFS5, PHLDA1, PLAC9, CRISPLD2, CSRP2, NOTCH3, CCDC102B, HIGD1B, RASD1, CRIP2, NR4A1, NDUFA4L2, UBN2, MTRNR2L8, ANGPTL4, MT2A, ITM2C, PDGFRB, SNCG, COX4I2, FABP5, ADIRF, COL1A2, CCL2
NASHaHSCsignature	IFITM1, MIF, COL1A1, S100A11, COL1A2, LGALS1, PDLIM3, LGALS3, SPON2, NNMT, NBEAL1, CTHRC1, VCAN, SERPINF1, COL3A1, SELM, MGP, CLEC11A, PPIB, PARK7, MTRNR2L12, TIMP1, FN1, FHL2, EMP3, COL5A1, IGFBP7, SERPINE1, NBL1, FAM127A, CRABP2, REXO2, MDK, MXRA8, LMNA, LRP1, SPARC, COL4A2, INAFM1, SPRY1, VIMP, PRDX4, TNFRSF12A, COX7A1, COL5A2, PHPT1, LXN, HCFC1R1, IGFBP6, PFDN4, PDLIM2, ARID5B, COL6A3, CD81, ISLR, ST3GAL4, PDGFRA, TMEM204, PYCR1, LTBP3, THY1

Note: The criteria for inclusion of genes in rHSCsignature or aHSCsignature were the log2 of fold change > 0.5 and adjusted *P* value < 0.05. The criteria for inclusion of genes in NASHrHSCsignature or NASHaHSCsignature were the log2 of fold change > 0.3 and *P* value < 0.05. Genes with significant findings in other relevant cell subsets were not included. Full names of those gene symbols were shown in the supplementary document.

Supplementary Fig. 1 shows the genes that were highly expressed in each cell subpopulation in the scRNA-seq analyses (Supplementary Fig. 1).

To verify whether the above-mentioned transcriptomic signatures can be used to define the corresponding HSC subsets, we evaluated the enrichment of the above two transcriptomic signatures in liver tissue of GSM4041162 using GSVA (Supplementary Fig. 2). As shown in Supplementary Fig. 2, rHSCsignature significantly enriched in rHSCs cluster but not in other cell clusters, indicating that the rHSCsignature can be used to represent rHSCs. aHSCsignature significantly enriched in aHSCs cluster but not in other cell clusters, indicating that the aHSCsignature can be used to represent aHSCs (Supplementary Fig. 2).

Single-cell transcriptomics identified NASH-specific transcriptomic signatures in both rHSC and aHSCs

We identified the genes abnormally changed in each HSC subset of NASH patients through scRNA-seq analysis (Fig. 2A and B). As shown in Fig. 2, aHSCs in NASH patients expressed higher levels of IFITM1, MIF, COL1A1, COL1A2, COL3A1, etc. than aHSCs in controls, and rHSCs in NASH patients expressed higher levels of ID3, NOTCH3, CRIP1, etc. than rHSC in controls (Table 1). Single-cell transcriptomics of HSCs reveled that aHSCs and rHSCs both existed in the liver tissues of NASH patients and healthy controls, but there was an obviously increased transition from rHSCs to aHSCs in NASH patients (Fig. 3A). Based on the above findings, we established NASH-associated transcriptomic signature of rHSC (NASHrHSCsignature) and NASH-associated transcriptomic signature of activated HSC (NASHaHSCsignature), respectively (Table 1). GSVA validated that NASHaHSCsignature obviously enriched in the aHSCs cluster of NASH patients, and NASHrHSCsignature obviously enriched in the rHSCs cluster of NASH patients, suggesting that the above two transcriptomic signatures could represent the respective cell subpopulations well (Fig. 3B and C). For instance, NASHaHSCsignature was significantly enriched in aHSCs in NASH patients but not in other cell subpopulations, suggesting that this transcriptomic signature can be used to represent NASH-associated aHSCs (Fig. 3B and C).

In addition, we also used transcriptomic data of HSCs stimulated by TGF-β (GSE148849) to assess the changes of those transcriptomic signatures above in HSCs activation. GSEA validated that NASHaHSCsignature was significantly increased in TGF-β-induced HSCs activation (Fig. 4A and B). Moreover, the enrichment score of NASHaHSCsignature calculated by GSVA was significantly increased in TGF-β-induced HSCs activation (Fig. 4C). The above outcomes suggested that NASHaHSCsignature could represent the activation state of HSCs.

https://ec.bioscientifica.com
https://doi.org/10.1530/EC-22-0502

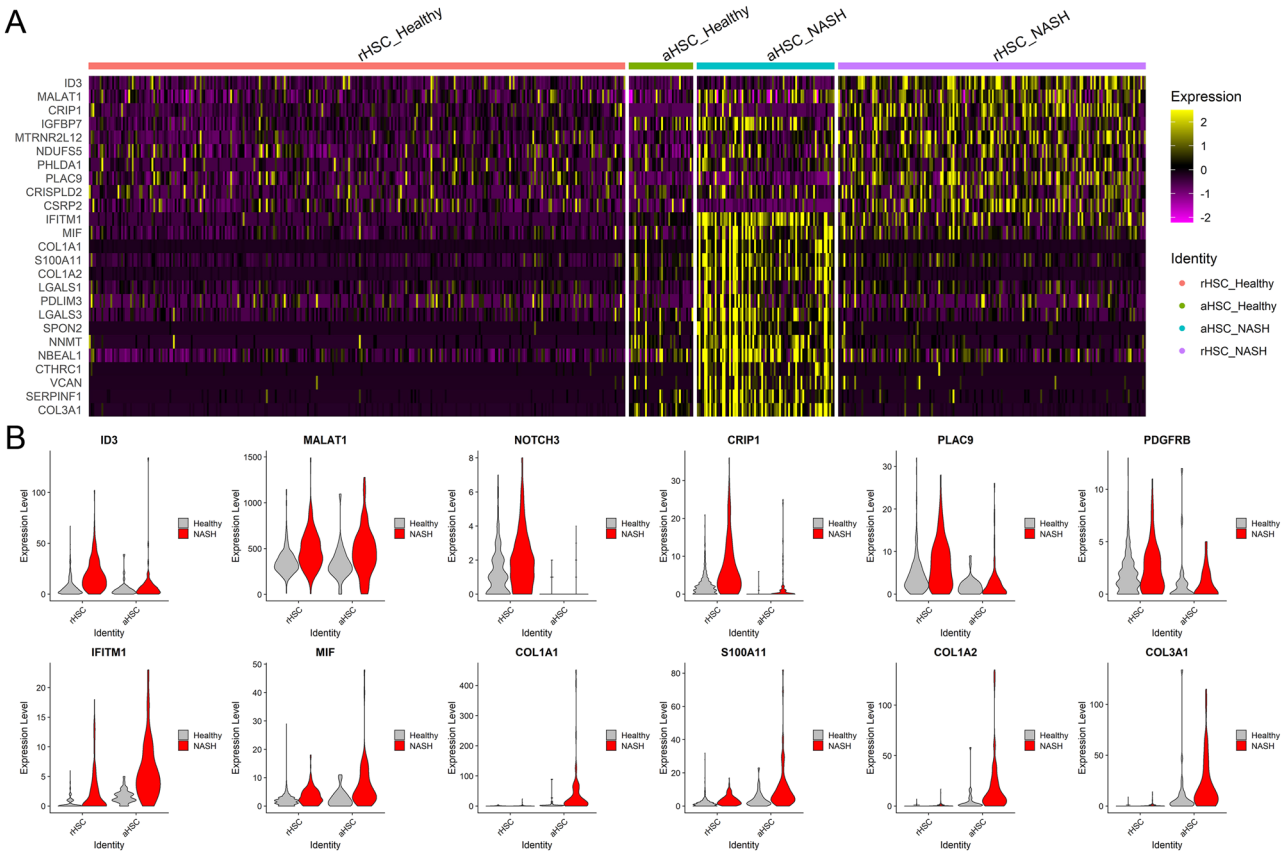

Figure 2

Establishment of NASH-associated transcriptomic signatures of activated HSCs and resting HSCs by single-cell RNA-sequencing analysis (A, Heat map showing the expressions of key signature genes in activated HSCs and resting HSCs from NASH patients or healthy controls; B, Violin plots showing the expressions of key signature genes in activated HSCs and resting HSCs from NASH patients or healthy controls).

We further validated the enrichment of NASHaHSCsignature in liver tissues of NASH patients or NAFLD patients with advanced fibrosis using the results of our previous study. We found that NASHaHSCsignature was significantly enriched in the liver of NASH patients and NAFLD patients with advanced fibrosis (Fig. 4D and E). It is further illustrated that the enrichment score of NASHaHSCsignature could represent the severity of fibrosis in NAFLD. In addition, aHSCsignature was significantly enriched in NASH patients and NAFLD with advanced fibrosis patients, indicating an increased number of aHSCs in the liver of NASH patients and NAFLD patients with advanced fibrosis (Fig. 4D and E). As shown in Fig. 4F, GSEA enrichment plots showing the significantly increased enrichment of NASHaHSCsignature in the livers of patients with NASH and advanced fibrosis of NAFLD (Fig. 4F).

We next validated the increased enrichment of NASHaHSCsignature in the livers of NAFLD patients with advanced fibrosis in bulk transcriptomic data of GSE49541 and GSE130970, which included patients with NAFLD with or without fibrosis. As shown in Fig. 5, the enrichment scores of NASHaHSCsignature calculated by GSVA in NAFLD patients with advanced fibrosis were significantly higher than that in patients without or with mild fibrosis ($P < 0.05$; Fig. 5A). ROC analysis revealed that enrichment score of NASHaHSCsignature in patients with NAFLD could help to diagnose advanced fibrosis (Fig. 5B). The outcomes showed that NASHaHSCsignature could effectively predict the advanced fibrosis in NAFLD patients. However, NASHaHSCsignature had limited performance in predicting NASH progression among NAFLD patients (Fig. 5C and D). Moreover, using a NASH mice model and CCl4-included fibrosis mice model, we validated the existence of rHSCs (mainly expressing a-SMA) in the normal liver and the increased aHSCs (mainly expressing collagen 1) in the fibrosis liver tissues (Fig. 6 and 7, Supplementary Fig. 3 and 4).

https://ec.bioscientifica.com
https://doi.org/10.1530/EC-22-0502

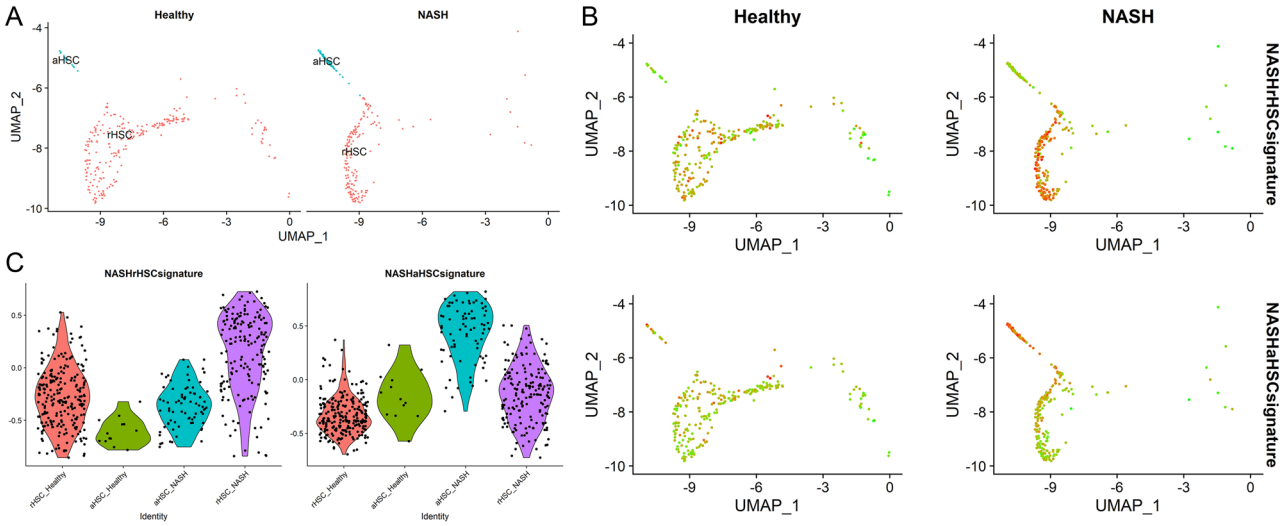

Figure 3
Validation of NASH-associated transcriptomic signatures of activated HSCs and resting HSCs by single-cell RNA-sequencing analysis (A, UMAP plot showing comparative analysis of the clusters in activated HSCs and resting HSCs between NASH and healthy controls; B, GSVA revealed that NASHaHSCsignature obviously enriched in the aHSCs cluster of NASH patients, and NASHrHSCsignature obviously enriched in the rHSCs cluster of NASH patients; C, Comparison of the enrichment scores of NASHaHSCsignature and NASHrHSCsignature in each HSCs cluster of NASH patients and healthy controls by violin plots).

Crucial functional pathways involved in the increased transition from rHSCs to aHSCs in NAFLD patients

To uncover those key genes and functional pathways involved in the increased transition from rHSCs to aHSCs in NAFLD patients, we performed WGCNA analyses of liver transcriptome data in NAFLD patients, in which the enrichment scores of HSCs-relevant transcriptomic signatures were used as clinical traits. Crucial co-expression modules correlated with the enrichment scores of HSCs-relevant transcriptomic signatures were thus explored by WGCNA analyses. As shown in Fig. 8, the co-expression pattern of genes in the liver transcriptome data of NAFLD patients was successfully constructed. The most significant co-expression module correlated with the enrichment score of NASHaHSCsignature was Memagenta module (correlation coefficient = 0.76, P = 2.0E-11), followed by Meturquoise (correlation coefficient = 0.44, P = 0.001) and Megreenyellow module (correlation coefficient = 0.43, P = 0.001). The MEmagenta co-expression module was also associated with advanced fibrosis (correlation coefficient = 0.85, P = 5.0E-16) and aHSCsignature enrichment score (correlation coefficient = 0.87, P = 5.0E-18) (Fig. 8B). Functional annotation analysis of Memagenta module showed that its functions were characterized by multiple ECM-related pathways such as extracellular matrix, extracellular matrix assembly, and extracellular structural organization (Fig. 8D). Functional annotation analysis of MEgreenyellow and MEturquoise co-expression modules showed that their functions were both characterized by immune response-related pathways (Supplementary Fig. 5). Thus, WGCNA analysis confirmed that ECM-related pathways and immune-related pathways were the main functional pathways involved in the activation of HSCs during NAFLD progression.

Key regulators involved in the transcriptomic change of aHSCs in NASH

We further explored those key regulators or transcription factor analyses for determining the functional change of aHSCs in NASH. As shown in Supplementary Fig. 6A, several key upstream regulators for determining the functional change of aHSCs in NASH were identified such as SDC1, GRP, SDC4, and MUC1. In the transcription factor enrichment analysis, some enriched transcription factor motifs, transcription factors, and their corresponding target genes were identified (Supplementary Table 3). For example, JAZF1 and FOBL1 could regulate the expressions of more than 40 genes upregulated in the aHSCs of NASH patients (Supplementary Fig. 6B). In addition, we found that JunB was one of the most critical transcription factors in NASH-associated aHSC and could regulate the expressions of many signature genes in NASHaHSCsignature

https://ec.bioscientifica.com
https://doi.org/10.1530/EC-22-0502

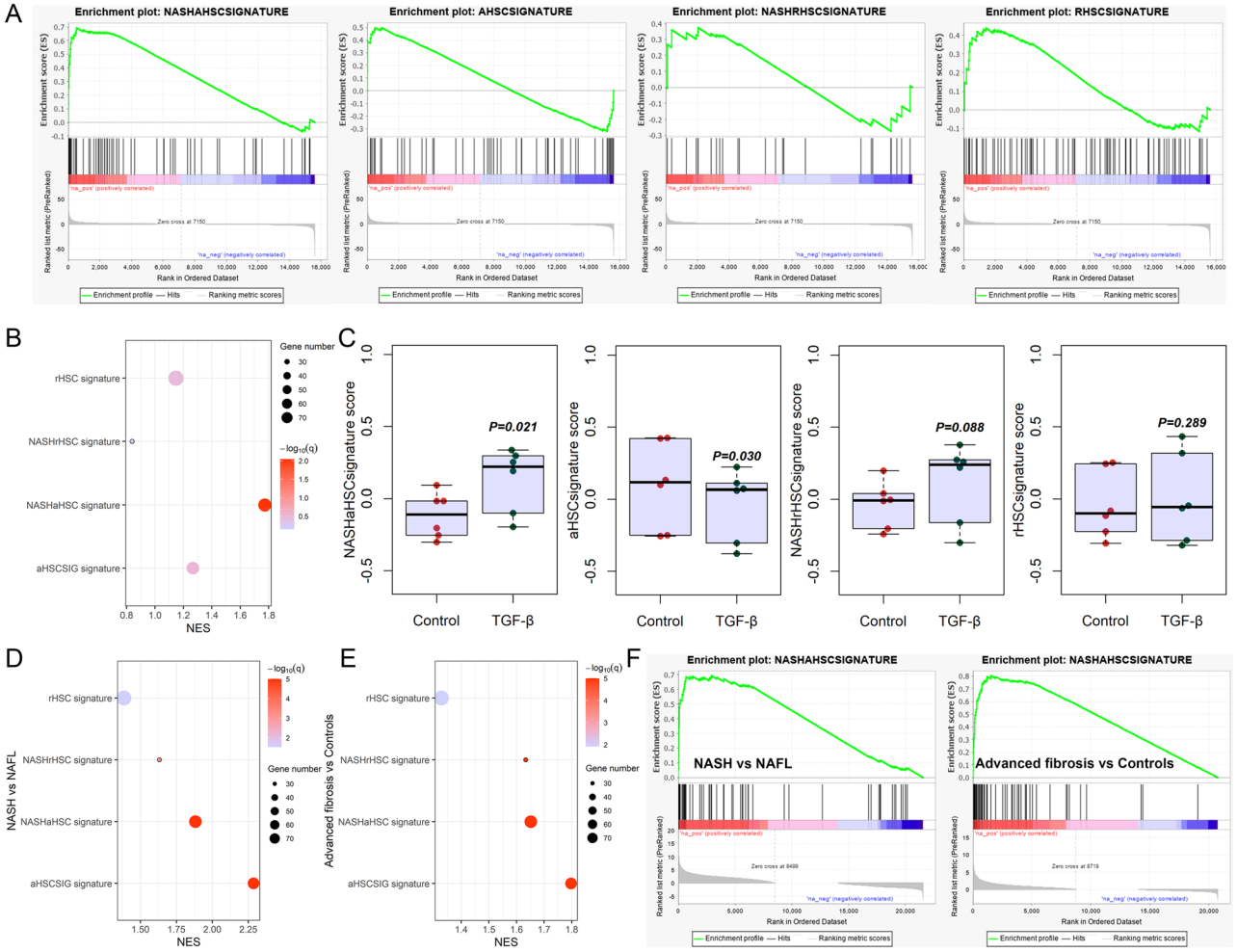

Figure 4

NASHaHSCsignature was significantly increased in TGF-β-induced HSCs activation and NASH progression and fibrosis of NAFLD patients (A, GSEA analyses validated the significantly increased enrichment of NASHaHSCsignature in TGF-β-induced HSCs activation; B, Bubble plot showing the enrichment of those signature gene sets during TGF-β-induced HSCs activation; C, Difference in the enrichment scores of the above signature gene sets in each HSC sample calculated by GSVA between TGF-β and control groups; D, Bubble plot showing the enrichment of those signature gene sets in the livers of patients with NASH progression; E, Bubble plot showing the enrichment of those signatures in the livers of NAFLD patients with advanced fibrosis; F, GSEA enrichment plots showing the significantly increased enrichment of NASHaHSCsignature in the livers of patients with NASH progression (left) or advanced fibrosis (right)).

(Supplementary Table 3). We used GSE148849, a transcriptomic dataset of HSC stimulated by TGF-β *in vitro*, to assess the change of JunB during HSCs activation, and we found that the expression of JunB in primary HSCs was significantly increased after TGF-β stimulation ($P = 0.008$) (Supplementary Fig. 7).

Correlation between key signatures and fibrosis severity of NAFLD patients

We validated the findings with a liver-sequencing dataset containing 206 patients with NAFLD and further evaluated the clinical significance of key transcriptomic signatures (GSE135251). The results showed that the GSVA enrichment scores of aHSCsignature and NASHaHSCsignature were significantly increased in NASH patients ($P < 0.05$) (Supplementary Fig. 8). GSVA enrichment scores of aHSCsignature and NASHaHSCsignature were significantly increased in the high NAS group (NAS 5–8) than the low NAS group (NAS 1–4) ($P < 0.001$) (Supplementary Fig. 9), and both signature enrichment scores increased with the increase of the severity of NAFLD patients ($P < 0.05$) (Supplementary Fig. 10). The GSVA enrichment scores of aHSCsignature and NASHaHSCsignature both increased significantly with the fibrosis severity of NAFLD patients (Supplementary Fig. 11 and 12). The findings suggested that changes in these HSCs-related signatures were able

https://ec.bioscientifica.com
https://doi.org/10.1530/EC-22-0502

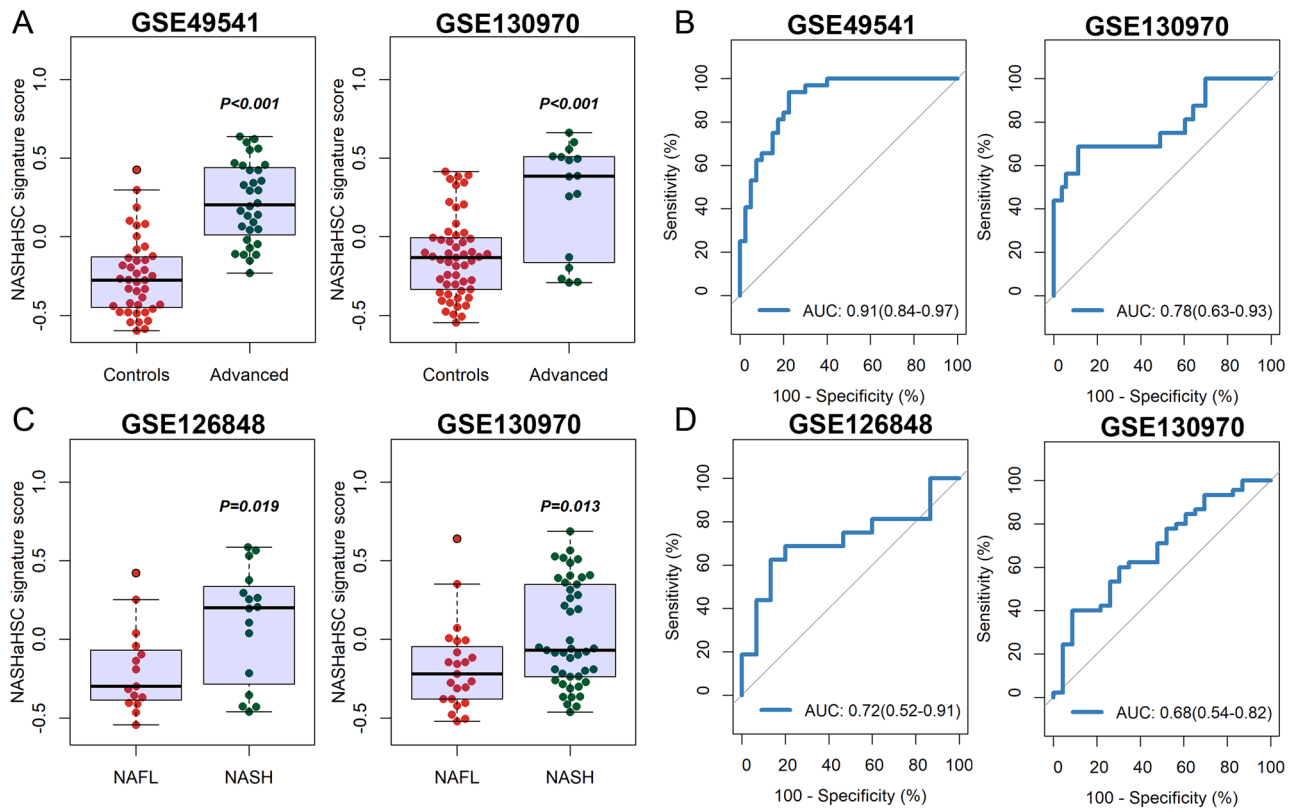

Figure 5
Validation of the increased enrichment of NASHaHSCsignature in the livers of NAFLD patients with advanced fibrosis (A, Difference in the enrichment scores of NASHaHSCsignature calculated by GSVA between patients with advanced fibrosis and controls; B, ROC analysis revealed enrichment score of NASHaHSCsignature in patients with NAFLD could help to diagnose advanced fibrosis; C, Difference in the enrichment scores of NASHaHSCsignature calculated by GSVA between NAFL patients and NASH patients; D, ROC analysis of GSVA enrichment scores of NASHaHSCsignature in patients with NAFL and NASH).

to show a progressive increase in the progression of liver fibrosis as well as NASH progression in common NAFLD patients. In addition, we analyzed the correlation between the expression of the top ten upregulated genes in aHSCsignature and NASHaHSCsignature and the severity of liver fibrosis in NAFLD patients (Supplementary Table 4). The results showed that the expressions of many genes were significantly correlated with the severity of liver fibrosis in NAFLD patients, but several genes were not significantly correlated with the severity of liver fibrosis. Therefore, the transcriptomic signatures had better performance in assessing the severity of fibrosis in NAFLD patients compared to single gene (Supplementary Table 4).

Discussion

Fibrosis in NASH is driven by the activation of HSCs, which transform from quiescent HSCs to myofibroblasts that produce collagen and other types of extracellular matrix (32, 33). Activated HSCs, as the source of hepatic myofibroblasts in NASH, are the most critical factor in producing excessive ECM and causing advanced fibrosis in the liver of NASH patients (22). This study was performed to identify transcriptomic signature of HSCs during the development of NASH and the underlying key functional pathways. This study defined the NASH-associated transcriptomic change of aHSCs and developed a useful transcriptomic signature with the potential .in assessing the fibrosis severity in the development of NASH. This study also identified extracellular matrix-related pathways and immune-related pathways as key players in the activation of HSCs during the development of NASH. Therefore, this study identified NASH-associated transcriptomic signature of HSC and provided new insights into fibrosis progression of NAFLD.

Our study identified differentially expressed genes in rHSC and aHSCs based on single-cell sequencing data and successfully established rHSCsignature and

https://ec.bioscientifica.com
https://doi.org/10.1530/EC-22-0502

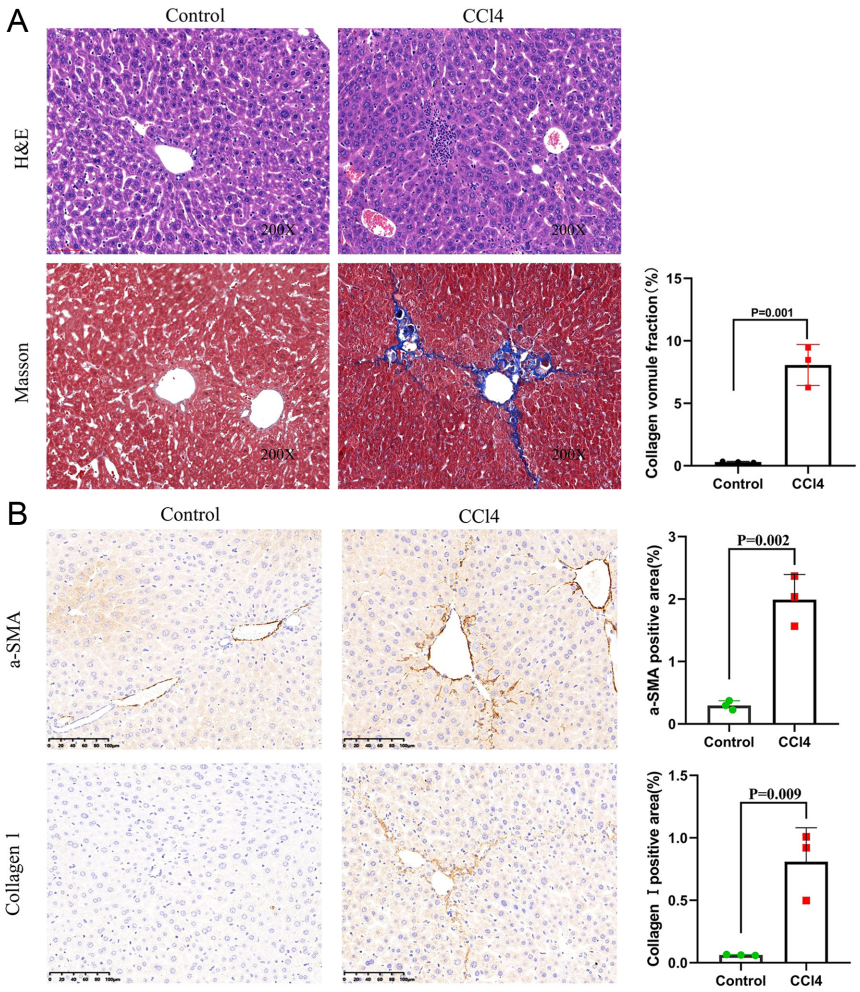

Figure 6
Expression of collagen 1 was significantly increased in areas of advanced fibrosis in liver tissue of CCl4-induced DBA/2J mice (A, Representative images of liver sections stained by H&E and Masson staining from control and mice of CCl4-induced liver fibrosis (original magnification, ×200); B, Immunohistochemistry of a-SMA and Collagen 1 expression in each group).

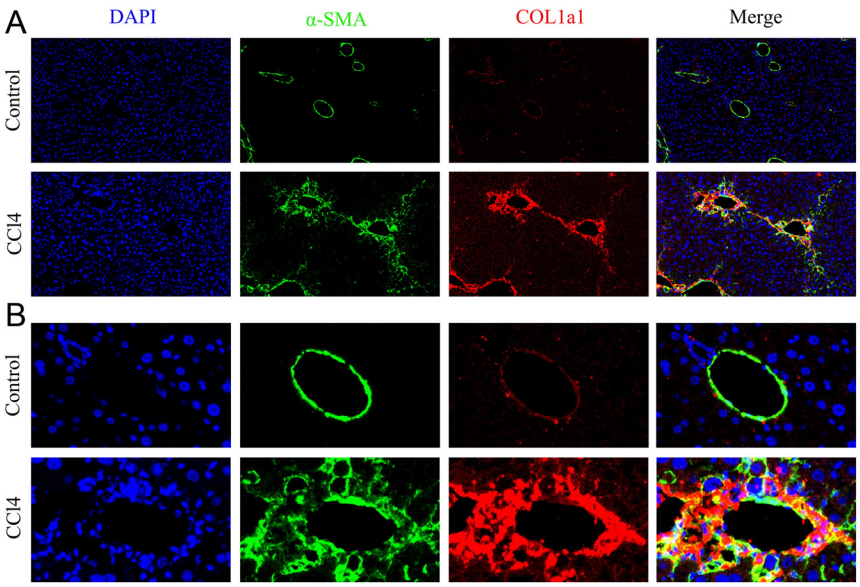

Figure 7
Change of expression of a-SMA and collagen 1 in control and mice of CCl4-induced liver fibrosis by immunofluorescence in DBA/2J mice (A, Representative images of liver sections stained by immunofluorescence from control and mice of CCl4-induced liver fibrosis (original magnification, ×50); B, Representative images of liver sections stained by immunofluorescence from control and mice of CCl4-induced liver fibrosis (original magnification, ×200)).

https://ec.bioscientifica.com
https://doi.org/10.1530/EC-22-0502

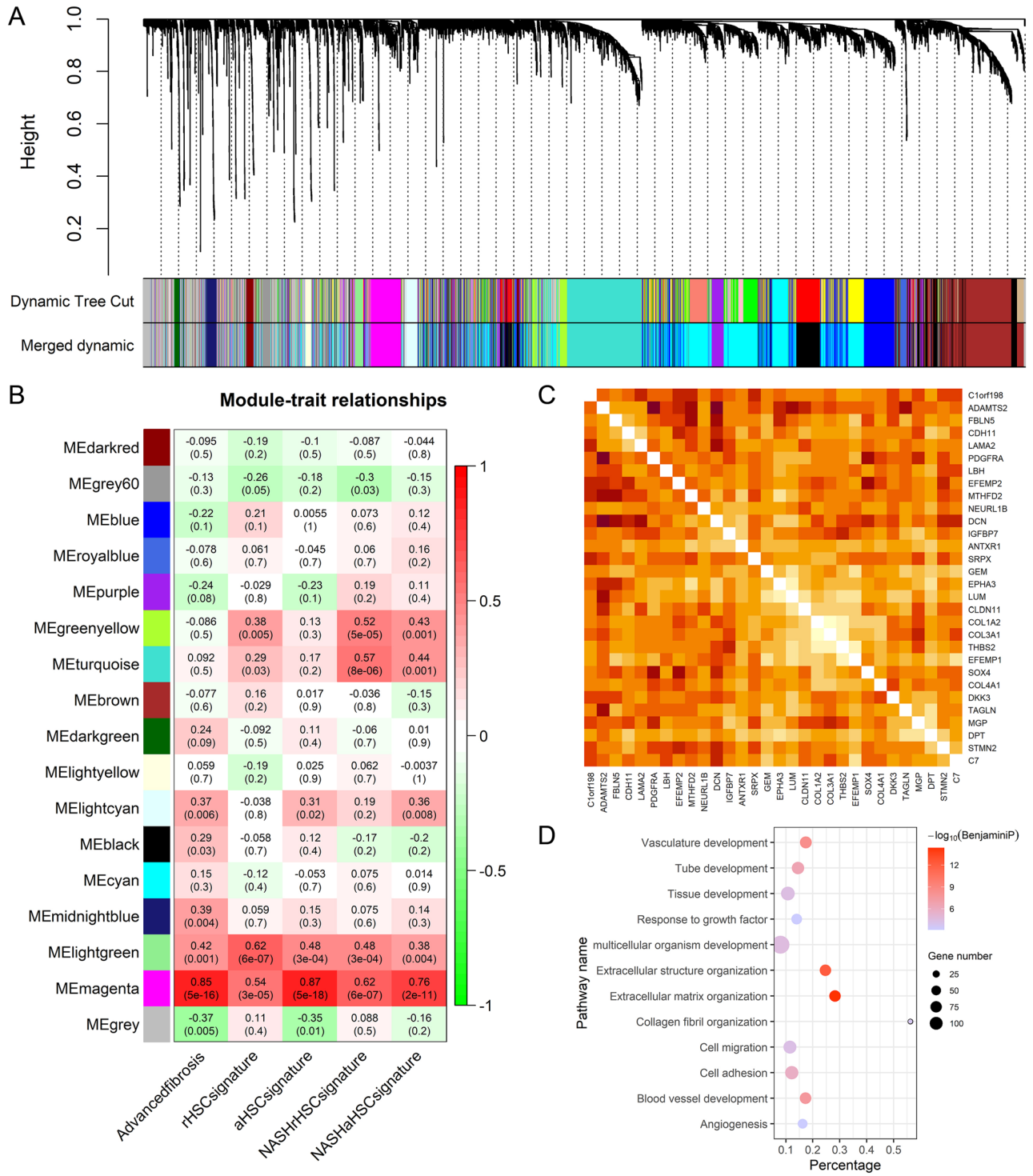

Figure 8

WGCNA identified crucial functional pathways involved in the increased transition from rHSCs to aHSCs in NAFLD patients (A, Clustering dendrogram showed the co-expression pattern of genes in the liver transcriptome data of NAFLD patients, in which each co-expression gene module was marked with one specific color; B, The heatmap showed the module-trait relationship identified in the WGCNA analysis, in which the coefficient and *P* values were presented and the transition from green to red indicated the increase in statistical significance; C, The hub genes in Memagenta module were intensively correlated with each other; D, Bubble plot showed those enriched pathways of genes in the MEmagenta co-expression module).

https://ec.bioscientifica.com
https://doi.org/10.1530/EC-22-0502

aHSCsignature, respectively. We then defined the NASH-associated transcriptomic changes of aHSCs and developed a useful transcriptomic signature with the potential of representing the degree of HSCs activation and fibrosis severity in NASH. NASHaHSCsignature was significantly enriched during TGF-β-stimulated HSCs activation *in vitro*, indicating that NASHaHSCsignature could represent the degree of HSCs activation. NASHaHSCsignature also had a strong diagnostic significance in assessing the severity of fibrosis of patients with NAFLD.

Many of those genes in aHSCsignature and NASHaHSCsignature have been reported to be closely associated with extracellular matrix and fibrosis. For instance, Lumican, encoded by LUM, has a key role in collagen assembly (34), and the formation of collagen fibers in the extracellular matrix of several tissues is regulated by lumican (35, 36, 37). Data presented by Anuradha Krishnan *et al.* suggest that lumican plays an important role in the progression of liver fibrosis by maintaining the stability of collagen fibers during fibrosis (38). Dermatopontin (DPT) has been shown to modulate collagen and fibrin fiber formation, induce cell adhesion, and promote wound healing (39, 40, 41). There is a study that found that the expression of DPT is positively correlated with the severity of liver fibrosis (42). ASPN plays a key role in tissue injury and regeneration (43). It has been found that ASPN expression is increased in the mouse model of pulmonary fibrosis, and ASPN is mainly localized in α-SMA$^+$ myofibroblasts. *In vitro* experiments demonstrated that ASPN knockout inhibited myofibroblast differentiation (43). However, the mechanisms of other signature genes in the fibrosis of NAFLD patients are unclear and still need to be investigated by more studies.

Apart from ECM-related pathways, we found that immune-related pathways were also key functional pathways involved in the activation of HSCs during NASH progression. There is emerging evidence supporting that innate and adaptive immune activation is the driving force in establishing liver inflammation and fibrosis in NASH (44). Some previous studies have found that immune cells or cytokines have important roles in the development of inflammation and liver fibrosis in NASH (45). In the liver tissue of NAFLD patients, immune cells such as monocytes and macrophages are involved in inflammation, thus promoting the progression of NAFLD to NASH (46, 47, 48). Therefore, immune-related pathways have key roles in the activation of HSCs during NASH progression and may be promising treatment targets.

Our study provides useful information for clinical evaluation of activated HSCs in NASH patients and may help to improve the diagnosis and risk stratification of fibrosis. Activated HSCs are the main effector cells of liver fibrosis and can produce excess extracellular matrix through chronic liver injury. The NASHaHSCsignature developed in our study can represent the degree of HSCs activation and has a strong diagnostic significance for the severity of NAFLD with fibrosis. It may help clinicians to determine the risk of developing liver fibrosis in the future and help to take early interventions to inhibit or delay the development of fibrosis among NAFLD patients.

Key upstream regulators or transcription factors related to the functional changes of HSCs are potential treatment targets for liver fibrosis of NASH patients. In this study, we tried to uncover those key regulators or transcription factor analyses for determining the functional change of aHSCs in NASH by two bioinformatic methods. Several key upstream regulators related to the functional changes of HSCs in NASH were identified such as SDC1, GRP, SDC4, and MUC1. SDC1 encodes heparan sulfate proteoglycan syndecan-1, which has been reported to be positively associated with liver fibrosis in patients with chronic liver diseases (49, 50). Knockdown of syndecan-1 could reduce the proliferation of keloid fibroblasts and the production of ECM (51). Another study by Parimon *et al.* found that syndecan-1 was a pro-fibrotic signal and could promote lung fibrosis by reprogramming the phenotypes of alveolar type II cells via augmenting TGF-β and Wnt signaling (52). The findings above suggest that syndecan-1 encoded by SDC1 may be a key regulator involving in liver fibrosis and a potential treatment target. In addition, JunB was found to be one of the most critical transcription factors in NASH-associated aHSC and could regulate the expressions of many signature genes in NASHaHSCsignature (Supplementary Table 3). JunB belongs to the JUN transcription factor family, including JunD and c-Jun, and can bind with Fos family and other transcription factors to form AP-1 dimer, which is a key transcription factor regulating cell survival and death pathways (53). It is also involved in various cellular processes such as proliferation, differentiation, apoptosis, transformation, cell migration, inflammation, and wound healing (54). Increasingly, JunB has also been found to play an important role in fibrogenesis, and JunB activates the TGF-β pathway and promotes COL1A2 deposition (55, 56, 57). In this study, we found that the expression of JunB in primary HSCs was significantly increased after

https://ec.bioscientifica.com
https://doi.org/10.1530/EC-22-0502

TGF-β stimulation. Therefore, JunB may be involved in the progression of liver fibrosis in NASH patients. The roles of other predicted upstream regulators or transcription factors in liver fibrosis of NASH patients are largely unclear. Further studies are recommended to explore the roles of those predicted upstream regulators or transcription factors in NASH and determine whether they are potential treatment targets against liver fibrosis in NASH.

Compared to previous literature, our study added novel insights into the fibrosis of NAFLD. We found that the transcriptomic signatures had better performance in assessing the severity of fibrosis in NAFLD patients compared to single gene. Moreover, the findings from a validation study suggested that changes in these HSCs-related signatures were able to show a progressive increase with the progression of liver fibrosis as well as NASH progression in NAFLD patients, suggesting the potential role of those transcriptional signatures in the evaluation and risk stratification for liver fibrosis in NAFLD.

There are some limitations in our study. First, the sample size of scRNA-seq studies is usually small because of the high cost of scRNA-seq, and it is the same with our study. The findings from this scRNA-seq study of small sample size can be validated by scRNA-seq studies with more samples. Secondly, for the potential upstream regulators, no causality could be confirmed by bioinformatic outcomes, and further experiments need to be performed to provide empirical evidence validating their involvement. Finally, the clinical significance of those transcriptional signatures in the diagnosis or management of NAFLD need to be explored with further prospective cohort studies or randomized controlled trials.

In summary, this study defined the NASH-associated transcriptomic changes of activated HSCs and developed a useful transcriptomic signature with the potential of representing the degree of HSCs activation and fibrosis severity in NASH. This study also identified extracellular matrix-related pathways and immune-related pathways as possible key players in the activation of HSCs during the development of NASH.

Supplementary materials

This is linked to the online version of the paper at https://doi.org/10.1530/EC-22-0502.

Declaration of interest

The authors declare that they have no conflict of interest.

Funding

This study was supported by the National Natural Science Foundation of China (No. 81870606) and the Natural Science Foundation of Fujian Province (2019J01569; 2021J011344).

Ethics approval

The study was approved by the Ethics Committee of the First Affiliated Hospital of Xiamen University (Ethics Number: 2021J011344).

Authors contribution statement

Xuejun Li and Weiwei He conceived of the paper; Weiwei He and Caoxin Huang wrote the original draft; Xiulin Shi, Menghua Wu and Han Li generated the figures; Qiuhong Liu, Xiaofang Zhang and Yan Zhao reviewed and edited the paper. All the authors agreed to the published version of the manuscript.

Acknowledgement

The authors would like to thank all the researchers who have shared their data in GEO database.

References

1 Sheka AC, Adeyi O, Thompson J, Hameed B, Crawford PA & Ikramuddin S. Nonalcoholic steatohepatitis: a review. *JAMA* 2020 **323** 1175–1183. (https://doi.org/10.1001/jama.2020.2298)

2 Younossi ZM. Non-alcoholic fatty liver disease - a global public health perspective. *Journal of Hepatology* 2019 **70** 531–544. (https://doi.org/10.1016/j.jhep.2018.10.033)

3 Younossi Z, Anstee QM, Marietti M, Hardy T, Henry L, Eslam M, George J & Bugianesi E. Global burden of NAFLD and NASH: trends, predictions, risk factors and prevention. *Nature Reviews. Gastroenterology and Hepatology* 2018 **15** 11–20. (https://doi.org/10.1038/nrgastro.2017.109)

4 Nalbantoglu IL & Brunt EM. Role of liver biopsy in nonalcoholic fatty liver disease. *World Journal of Gastroenterology* 2014 **20** 9026–9037. (https://doi.org/10.3748/wjg.v20.i27.9026)

5 Farrell GC & Larter CZ. Nonalcoholic fatty liver disease: from steatosis to cirrhosis. *Hepatology* 2006 **43**(Supplement 1) S99–S112. (https://doi.org/10.1002/hep.20973)

6 Hardy T, Oakley F, Anstee QM & Day CP. Nonalcoholic fatty liver disease: pathogenesis and disease spectrum. *Annual Review of Pathology* 2016 **11** 451–496. (https://doi.org/10.1146/annurev-pathol-012615-044224)

7 Noureddin M, Vipani A, Bresee C, Todo T, Kim IK, Alkhouri N, Setiawan VW, Tran T, Ayoub WS, Lu SC, *et al.* NASH leading cause of liver transplant in women: updated analysis of indications for liver transplant and ethnic and gender variances. *American Journal of Gastroenterology* 2018 **113** 1649–1659. (https://doi.org/10.1038/s41395-018-0088-6)

8 Younossi ZM, Tampi R, Priyadarshini M, Nader F, Younossi IM & Racila A. Burden of illness and economic model for patients with nonalcoholic steatohepatitis in the United States. *Hepatology* 2019 **69** 564–572. (https://doi.org/10.1002/hep.30254)

9 Mikolasevic I, Filipec-Kanizaj T, Mijic M, Jakopcic I, Milic S, Hrstic I, Sobocan N, Stimac D & Burra P. Nonalcoholic fatty liver disease and liver transplantation: where do we stand? *World Journal of Gastroenterology* 2018 **24** 1491–1506. (https://doi.org/10.3748/wjg.v24.i14.1491)

10 Angulo P, Kleiner DE, Dam-Larsen S, Adams LA, Bjornsson ES, Charatcharoenwitthaya P, Mills PR, Keach JC, Lafferty HD, Stahler A, *et al.* Liver fibrosis, but no other histologic features, is associated with

long-term outcomes of patients with nonalcoholic fatty liver disease. *Gastroenterology* 2015 **149** 389–97.e10. (https://doi.org/10.1053/j.gastro.2015.04.043)
11 Hagstrom H, Nasr P, Ekstedt M, Hammar U, Stal P, Hultcrantz R & Kechagias S. Fibrosis stage but not NASH predicts mortality and time to development of severe liver disease in biopsy-proven NAFLD. *Journal of Hepatology* 2017 **67** 1265–1273. (https://doi.org/10.1016/j.jhep.2017.07.027)
12 Kim GA, Lee HC, Choe J, Kim MJ, Lee MJ, Chang HS, Bae IY, Kim HK, An J, Shim JH, *et al.* Association between non-alcoholic fatty liver disease and cancer incidence rate. *Journal of Hepatology* 2017 **68** P140–146. (https://doi.org/10.1016/j.jhep.2017.09.012)
13 Dulai PS, Singh S, Patel J, Soni M, Prokop LJ, Younossi Z, Sebastiani G, Ekstedt M, Hagstrom H, Nasr P, *et al.* Increased risk of mortality by fibrosis stage in nonalcoholic fatty liver disease: systematic review and meta-analysis. *Hepatology* 2017 **65** 1557–1565. (https://doi.org/10.1002/hep.29085)
14 Vilar-Gomez E, Calzadilla-Bertot L, Wai-Sun WV, Castellanos M, Aller-de la Fuente R, Metwally M, Eslam M, Gonzalez-Fabian L, Sanz A-Q, Conde-Martin AF, *et al.* Fibrosis severity as a determinant of cause-specific mortality in patients with advanced nonalcoholic fatty liver disease: a multi-national cohort study. *Gastroenterology* 2018 **155** 443–457.e417. (https://doi.org/10.1053/j.gastro.2018.04.034)
15 Friedman SL, Neuschwander-Tetri BA, Rinella M & Sanyal AJ. Mechanisms of NAFLD development and therapeutic strategies. *Nature Medicine* 2018 **24** 908–922. (https://doi.org/10.1038/s41591-018-0104-9)
16 Angulo P, Machado MV & Diehl AM. Fibrosis in nonalcoholic Fatty liver disease: mechanisms and clinical implications. *Seminars in Liver Disease* 2015 **35** 132–145. (https://doi.org/10.1055/s-0035-1550065)
17 Schwabe RF, Tabas I & Pajvani UB. Mechanisms of fibrosis development in nonalcoholic steatohepatitis. *Gastroenterology* 2020 **158** 1913–1928. (https://doi.org/10.1053/j.gastro.2019.11.311)
18 Karsdal MA, Manon-Jensen T, Genovese F, Kristensen JH, Nielsen MJ, Sand JM, Hansen NU, Bay-Jensen AC, Bager CL, Krag A, *et al.* Novel insights into the function and dynamics of extracellular matrix in liver fibrosis. *American Journal of Physiology. Gastrointestinal and Liver Physiology* 2015 **308** G807–G830. (https://doi.org/10.1152/ajpgi.00447.2014)
19 Friedman SL. Hepatic stellate cells: protean, multifunctional, and enigmatic cells of the liver. *Physiological Reviews* 2008 **88** 125–172. (https://doi.org/10.1152/physrev.00013.2007)
20 Mederacke I, Hsu CC, Troeger JS, Huebener P, Mu X, Dapito DH, Pradere JP & Schwabe RF. Fate tracing reveals hepatic stellate cells as dominant contributors to liver fibrosis independent of its aetiology. *Nature Communications* 2013 **4** 2823. (https://doi.org/10.1038/ncomms3823)
21 Xu J & Kisseleva T. Bone marrow-derived fibrocytes contribute to liver fibrosis. *Experimental Biology and Medicine* 2015 **240** 691–700. (https://doi.org/10.1177/1535370215584933)
22 Marcher AB, Bendixen SM, Terkelsen MK, Hohmann SS, Hansen MH, Larsen BD, Mandrup S, Dimke H, Detlefsen S & Ravnskjaer K. Transcriptional regulation of Hepatic Stellate Cell activation in NASH. *Scientific Reports* 2019 **9** 2324. (https://doi.org/10.1038/s41598-019-39112-6)
23 Wells RG & Schwabe RF. Origin and function of myofibroblasts in the liver. *Seminars in Liver Disease* 2015 **35** 97–106. (https://doi.org/10.1055/s-0035-1550061)
24 Higashi T, Friedman SL & Hoshida Y. Hepatic stellate cells as key target in liver fibrosis. *Advanced Drug Delivery Reviews* 2017 **121** 27–42. (https://doi.org/10.1016/j.addr.2017.05.007)
25 Stuart T, Butler A, Hoffman P, Hafemeister C, Papalexi E, Mauck WM, 3rd, Hao Y, Stoeckius M, Smibert P & Satija R. Comprehensive integration of single-cell data. *Cell* 2019 **177** 1888–1902.e21. (https://doi.org/10.1016/j.cell.2019.05.031)
26 Hanzelmann S, Castelo R & Guinney J. GSVA: gene set variation analysis for microarray and RNA-seq data. *BMC Bioinformatics* 2013 **14** 7. (https://doi.org/10.1186/1471-2105-14-7)
27 Subramanian A, Tamayo P, Mootha VK, Mukherjee S, Ebert BL, Gillette MA, Paulovich A, Pomeroy SL, Golub TR, Lander ES, *et al.* Gene set enrichment analysis: a knowledge-based approach for interpreting genome-wide expression profiles. *PNAS* 2005 **102** 15545–15550. (https://doi.org/10.1073/pnas.0506580102)
28 He W, Huang C, Zhang X, Wang D, Chen Y, Zhao Y & Li X. Identification of transcriptomic signatures and crucial pathways involved in non-alcoholic steatohepatitis. *Endocrine* 2021 **73** 52–64. (https://doi.org/10.1007/s12020-021-02716-y)
29 Presson AP, Sobel EM, Papp JC, Suarez CJ, Whistler T, Rajeevan MS, Vernon SD & Horvath S. Integrated weighted gene co-expression network analysis with an application to chronic fatigue syndrome. *BMC Systems Biology* 2008 **2** 95. (https://doi.org/10.1186/1752-0509-2-95)
30 Fakhry CT, Choudhary P, Gutteridge A, Sidders B, Chen P, Ziemek D & Zarringhalam K. Interpreting transcriptional changes using causal graphs: new methods and their practical utility on public networks. *BMC Bioinformatics* 2016 **17** 318. (https://doi.org/10.1186/s12859-016-1181-8)
31 Janky R, Verfaillie A, Imrichova H, Van de Sande B, Standaert L, Christiaens V, Hulselmans G, Herten K, Naval Sanchez M, Potier D, *et al.* iRegulon: from a gene list to a gene regulatory network using large motif and track collections. *PLoS Computational Biology* 2014 **10** e1003731. (https://doi.org/10.1371/journal.pcbi.1003731)
32 Puche JE, Saiman Y & Friedman SL. Hepatic stellate cells and liver fibrosis. *Comprehensive Physiology* 2013 **3** 1473–1492. (https://doi.org/10.1002/cphy.c120035)
33 Tsuchida T & Friedman SL. Mechanisms of hepatic stellate cell activation. *Nature Reviews. Gastroenterology and Hepatology* 2017 **14** 397–411. (https://doi.org/10.1038/nrgastro.2017.38)
34 Rada JA, Cornuet PK & Hassell JR. Regulation of corneal collagen fibrillogenesis in vitro by corneal proteoglycan (lumican and decorin) core proteins. *Experimental Eye Research* 1993 **56** 635–648. (https://doi.org/10.1006/exer.1993.1081)
35 Brezillon S, Venteo L, Ramont L, D'Onofrio MF, Perreau C, Pluot M, Maquart FX & Wegrowski Y. Expression of lumican, a small leucine-rich proteoglycan with antitumour activity, in human malignant melanoma. *Clinical and Experimental Dermatology* 2007 **32** 405–416. (https://doi.org/10.1111/j.1365-2230.2007.02437.x)
36 Melrose J, Fuller ES, Roughley PJ, Smith MM, Kerr B, Hughes CE, Caterson B & Little CB. Fragmentation of decorin, biglycan, lumican and keratocan is elevated in degenerate human meniscus, knee and hip articular cartilages compared with age-matched macroscopically normal and control tissues. *Arthritis Research and Therapy* 2008 **10** R79. (https://doi.org/10.1186/ar2453)
37 Raouf A, Ganss B, McMahon C, Vary C, Roughley PJ & Seth A. Lumican is a major proteoglycan component of the bone matrix. *Matrix Biology* 2002 **21** 361–367. (https://doi.org/10.1016/s0945-053x(02)00027-6)
38 Krishnan A, Li X, Kao WY, Viker K, Butters K, Masuoka H, Knudsen B, Gores G & Charlton M. Lumican, an extracellular matrix proteoglycan, is a novel requisite for hepatic fibrosis. *Laboratory Investigation* 2012 **92** 1712–1725. (https://doi.org/10.1038/labinvest.2012.121)
39 Kato A, Okamoto O, Ishikawa K, Sumiyoshi H, Matsuo N, Yoshioka H, Nomizu M, Shimada T & Fujiwara S. Dermatopontin interacts with fibronectin, promotes fibronectin fibril formation, and enhances cell adhesion. *Journal of Biological Chemistry* 2011 **286** 14861–14869. (https://doi.org/10.1074/jbc.M110.179762)
40 Kato A, Okamoto O, Wu W, Matsuo N, Kumai J, Yamada Y, Katagiri F, Nomizu M & Fujiwara S. Identification of fibronectin binding sites in dermatopontin and their biological function. *Journal of Dermatological Science* 2014 **76** 51–59. (https://doi.org/10.1016/j.jdermsci.2014.07.003)

41 Wu W, Okamoto O, Kato A, Matsuo N, Kumai J, Nomizu M & Fujiwara S. Functional peptide of dermatopontin produces fibrinogen fibrils and modifies its biological activity. *Journal of Dermatological Science* 2014 **76** 34–43. (https://doi.org/10.1016/j.jdermsci.2014.07.002)

42 Li Y, Yuan SL, Yin JY, Yang K, Zhou XG, Xie W & Wang Q. Differences of core genes in liver fibrosis and hepatocellular carcinoma: evidence from integrated bioinformatics and immunohistochemical analysis. *World Journal of Gastrointestinal Oncology* 2022 **14** 1265–1280. (https://doi.org/10.4251/wjgo.v14.i7.1265)

43 Huang S, Lai X, Yang L, Ye F, Huang C, Qiu Y, Lin S, Pu L, Wang Z & Huang W. Asporin promotes TGF-beta-induced lung myofibroblast differentiation by facilitating Rab11-dependent recycling of TbetaRI. *American Journal of Respiratory Cell and Molecular Biology* 2022 **66** 158–170. (https://doi.org/10.1165/rcmb.2021-0257OC)

44 Dallio M, Sangineto M, Romeo M, Villani R, Romano AD, Loguercio C, Serviddio G & Federico A. Immunity as cornerstone of non-alcoholic fatty liver disease: the contribution of oxidative stress in the disease progression. *International Journal of Molecular Sciences* 2021 **22** 436. (https://doi.org/10.3390/ijms22010436)

45 Luci C, Bourinet M, Leclere PS, Anty R & Gual P. Chronic inflammation in non-alcoholic steatohepatitis: molecular mechanisms and therapeutic strategies. *Frontiers in Endocrinology (Lausanne)* 2020 **11** 597648. (https://doi.org/10.3389/fendo.2020.597648)

46 Luci C, Vieira E, Perchet T, Gual P & Golub R. Natural killer cells and type 1 innate lymphoid cells are new actors in non-alcoholic fatty liver disease. *Frontiers in Immunology* 2019 **10** 1192. (https://doi.org/10.3389/fimmu.2019.01192)

47 Cai J, Zhang XJ & Li H. The role of innate immune cells in nonalcoholic steatohepatitis. *Hepatology* 2019 **70** 1026–1037. (https://doi.org/10.1002/hep.30506)

48 Kazankov K, Jorgensen SMD, Thomsen KL, Moller HJ, Vilstrup H, George J, Schuppan D & Gronbaek H. The role of macrophages in nonalcoholic fatty liver disease and nonalcoholic steatohepatitis. *Nature Reviews. Gastroenterology and Hepatology* 2019 **16** 145–159. (https://doi.org/10.1038/s41575-018-0082-x)

49 Charchanti A, Kanavaros P, Koniaris E, Kataki A, Glantzounis G, Agnantis NJ & Goussia AC. Expression of Syndecan-1 in chronic liver diseases: correlation with hepatic fibrosis. *In Vivo* **2021 35** 333–339. (https://doi.org/10.21873/invivo.12264)

50 Zvibel I, Halfon P, Fishman S, Penaranda G, Leshno M, Or AB, Halpern Z & Oren R. Syndecan 1 (CD138) serum levels: a novel biomarker in predicting liver fibrosis stage in patients with hepatitis C. *Liver International* 2009 **29** 208–212. (https://doi.org/10.1111/j.1478-3231.2008.01830.x)

51 Cui J, Jin S, Jin C & Jin Z. Syndecan-1 regulates extracellular matrix expression in keloid fibroblasts via TGF-beta1/Smad and MAPK signaling pathways. *Life Sciences* 2020 **254** 117326. (https://doi.org/10.1016/j.lfs.2020.117326)

52 Parimon T, Yao C, Habiel DM, Ge L, Bora SA, Brauer R, Evans CM, Xie T, Alonso-Valenteen F, Medina-Kauwe LK, *et al.* Syndecan-1 promotes lung fibrosis by regulating epithelial reprogramming through extracellular vesicles. *JCI Insight* 2019 **5** e129359. (https://doi.org/10.1172/jci.insight.129359)

53 Papoudou-Bai A, Hatzimichael E, Barbouti A & Kanavaros P. Expression patterns of the activator protein-1 (AP-1) family members in lymphoid neoplasms. *Clinical and Experimental Medicine* 2017 **17** 291–304. (https://doi.org/10.1007/s10238-016-0436-z)

54 Piechaczyk M & Farras R. Regulation and function of JunB in cell proliferation. *Biochemical Society Transactions* 2008 **36** 864–867. (https://doi.org/10.1042/BST0360864)

55 Gervasi M, Bianchi-Smiraglia A, Cummings M, Zheng Q, Wang D, Liu S & Bakin AV. JunB contributes to Id2 repression and the epithelial-mesenchymal transition in response to transforming growth factor-beta. *Journal of Cell Biology* 2012 **196** 589–603. (https://doi.org/10.1083/jcb.201109045)

56 Ponticos M, Papaioannou I, Xu S, Holmes AM, Khan K, Denton CP, Bou-Gharios G & Abraham DJ. Failed degradation of JunB contributes to overproduction of type I collagen and development of dermal fibrosis in patients with systemic sclerosis. *Arthritis and Rheumatology* 2015 **67** 243–253. (https://doi.org/10.1002/art.38897)

57 Choudhuri S & Garg NJ. Trypanosoma cruzi Induces the PARP1/AP-1 Pathway for Upregulation of metalloproteinases and transforming growth factor beta in Macrophages: role in Cardiac Fibroblast Differentiation and Fibrosis in Chagas disease. *mBio* 2020 **11** e01853-20. (https://doi.org/10.1128/mBio.01853-20)

Received in final form 1 December 2022
Accepted 23 December 2022
Accepted Manuscript published online 23 December 2022